# Reducing the $H_0$ and $\sigma_8$ tensions with dark matter-neutrino interactions

Eleonora Di Valentino,[1,*] Céline Bœhm,[2,3,4,†] Eric Hivon,[5] and François R. Bouchet[5]

[1]*Jodrell Bank Center for Astrophysics, School of Physics and Astronomy, University of Manchester, Oxford Road, Manchester M13 9PL, United Kingdom*
[2]*Institute for Particle Physics Phenomenology, Durham University, South Road, Durham DH1 3LE, United Kingdom*
[3]*LAPTH, Universitaire de Savoie, CNRS, BP 110, 74941 Annecy-Le-Vieux, France*
[4]*Perimeter Institute, 31 Caroline Street North, Waterloo, Ontario, Canada N2L 2Y5*
[5]*Institut d'Astrophysique de Paris (UMR7095: CNRS & Sorbonne Université), F-75014 Paris, France*

(Received 13 October 2017; published 13 February 2018)

The introduction of dark matter-neutrino interactions modifies the cosmic microwave background (CMB) angular power spectrum at all scales, thus affecting the reconstruction of the cosmological parameters. Such interactions can lead to a slight increase of the value of $H_0$ and a slight decrease of $S_8 \equiv \sigma_8\sqrt{\Omega_m/0.3}$, which can help reduce somewhat the tension between the CMB and weak lensing or Cepheids data sets. Here we show that it is impossible to solve both tensions simultaneously. While the 2015 Planck temperature and low multipole polarization data combined with the Cepheids data sets prefer large values of the Hubble rate (up to $H_0 = 72.1^{+1.5}_{-1.7}$ km/s/Mpc, when $N_{\mathrm{eff}}$ is free to vary), the $\sigma_8$ parameter remains too large to reduce the $\sigma_8$ tension. Adding high multipole Planck polarization data does not help since this data shows a strong preference for low values of $H_0$, thus worsening current tensions, even though they also prefer smaller value of $\sigma_8$.

DOI: 10.1103/PhysRevD.97.043513

## I. INTRODUCTION

In the standard cosmological framework, dark matter is assumed to be collisionless. In practice this means that one arbitrarily sets the dark matter interactions to zero when predicting the angular power spectrum of the cosmic microwave background (CMB). However this treatment is at odds with the principle behind dark matter direct and indirect detection, where one explicitly assumes that dark matter (DM) interacts with ordinary matter. This is also in contradiction with the thermal hypothesis which relies on dark matter annihilations to explain the observed dark matter relic density.

A more consistent approach consists in accounting for dark matter interactions and test whether they can be neglected by looking at their effects on cosmological observables. DM interactions in the early Universe damp the primordial dark matter fluctuations through the collisional damping mechanism [1–3]. They also affect the evolution of the other fluid(s) which the DM is interacting with. The two effects simultaneously impact the distribution of light and matter in the early Universe [4] and eventually affect structure formation in the dark ages [5]. They can also modify how our own cosmic neighborhood should look like [6–10] and change the estimates of the cosmological parameters needed to account for the observed CMB anisotropies.

The so-called "cutoff" scale at which one notices departures from the Lambda + Cold DM model (LCDM) predictions in the matter power spectrum is governed by the ratio of the elastic scattering cross section (corresponding to the dark matter scattering off the species $i$, normalized to the Thomson cross section $\sigma_T$) to the dark matter mass. We refer to this ratio as

$$u_i = \frac{\sigma_{\mathrm{DM}-i}}{\sigma_T}\left(\frac{m_{\mathrm{DM}}}{100\ \mathrm{GeV}}\right)^{-1}.$$

The larger $u_i$, the higher the cutoff scale [2–4].

Dark matter-radiation interactions is the most interesting case among all interacting DM scenarios. Since radiation dominates the energy in the Universe for a very long time, such interactions erase the dark matter fluctuations on relatively large-scales for $u \ll 1$ and also change the way the CMB looks like across the sky [2–4,11–20]. Dark matter-baryon and dark matter self-interactions can also erase the DM fluctuations but the $u$ ratio needs to be of order 1 to produce the same effects as the one considered here [2,3], given that there are many less baryons than radiation in the Universe and baryons are nonrelativistic.

In what follows, we focus on dark matter-neutrino interactions and study their impact on the cosmological

*eleonora.divalentino@manchester.ac.uk
†c.m.boehm@durham.ac.uk

 

parameters (in particular the Hubble rate $H_0$, the effective number of relativistic degrees of freedom $N_{\rm eff}$ and the linear matter power spectrum value at 8 Mpc, $\sigma_8$). Previous analyses [21] indicated that dark matter-neutrino interactions prefer higher values of $H_0$ with respect to LCDM estimates. The higher $N_{\rm eff}$, the higher $H_0$. Therefore we investigate whether DM-$\nu$ interactions could at least partially solve the current tensions arising between the CMB and late-time (i.e., strong lensing [22] and Cepheids [23]) measurements of the $H_0$ value. We also study whether DM-$\nu$ interactions could reduce the tension between the CMB-inferred value of $\sigma_8$ and large-scale-structure surveys, owing to the damping they induce.

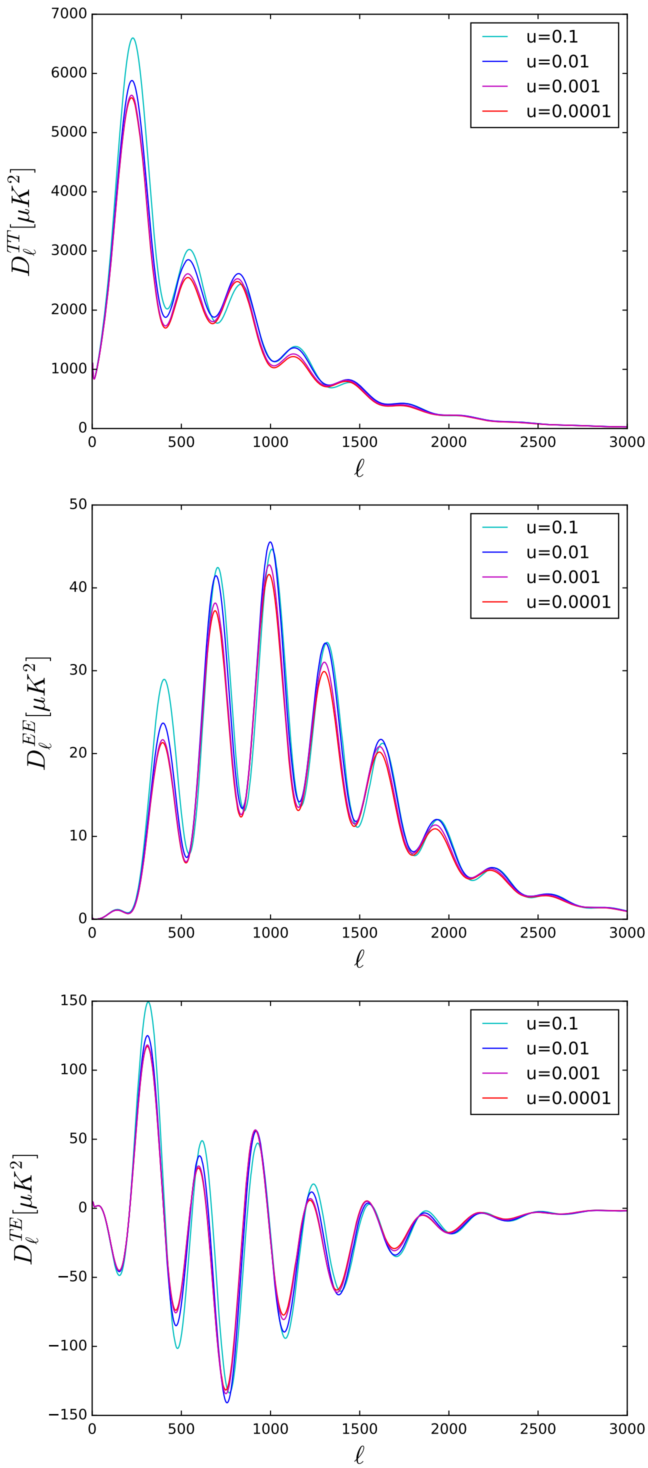


FIG. 1. The temperature and polarization CMB angular power spectra in the presence of dark matter-neutrino interactions.

In what follows, we consider the Planck 2015 data from the full mission duration, both the recommended temperature plus low multipole polarization information, as well as the complete spectral information, thereby including also the high multipole polarization information which the Planck team considers as preliminary due to the presence of small but detectable low level residual systematics of $\mathcal{O}(1)\ \mu K^2$ [24]. We briefly remind the reader of the expected impact of the DM interactions on the cosmological parameters in Sec. II. In Sec. III, we present the method used to analyze the data and give the results in Secs. IV, V, and VI. We conclude in Sec. VII.

## II. IMPACT OF THE DM-$\nu$ INTERACTIONS ON THE COSMOLOGICAL PARAMETERS

The dark matter-neutrino interactions have five distinct effects on the temperature and polarization angular power spectra. These were explained in Ref. [21] and can be seen in Fig. 1. The effect of the interactions on the lensing potential power spectrum are illustrated in Fig. 2.

Schematically, one can understand the impact of a DM-$\nu$ coupling on the cosmological parameters as follows. On one hand, the DM-$\nu$ interactions induce a damping of the DM fluctuations at small-scales (i.e., at high multipoles). On the other hand, they prevent the neutrino free-streaming, till the neutrinos kinetically decouple from the DM. This last effect enhances the peaks at low multipoles, where the CMB

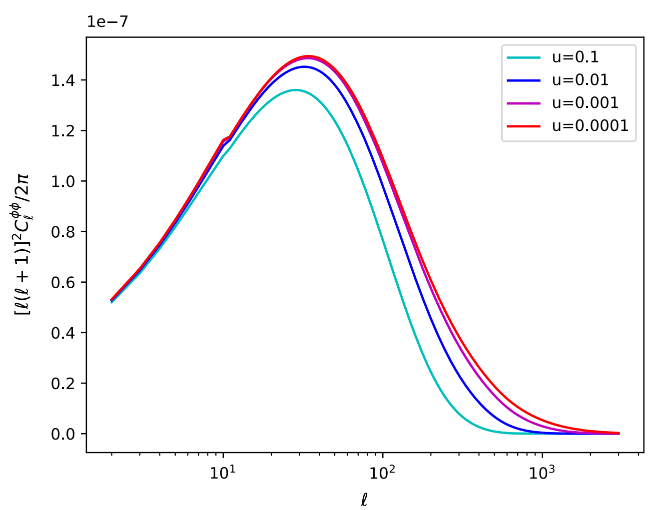


FIG. 2. The lensing potential power spectrum in the presence of dark matter-neutrino interactions.

temperature angular power spectrum is best measured. The greater the elastic scattering cross section (or the lighter the dark matter), the more pronounced are these two effects. Hence the fit to the data imposes an upper limit on the strength of these interactions.

The enhancement of the first few peaks is less pronounced in a younger Universe. Hence scenarios with DM-$\nu$ interactions are compatible with the data, when the value of $H_0$ is larger than the value estimated using the LCDM model. One should also observe a damping of the DM primordial fluctuations at small-scales because of the impact of neutrinos on the DM fluid. This effect translates into a damped oscillating matter power spectrum [4] and thus leads to a smaller value of the $\sigma_8$ parameter than that in the LCDM scenario.

Finally, we note that the difference in TE spectra between $u = 10^{-3}$ and $u = 10^{-4}$ is of the order of the same order of magnitude as Planck sensitivity (e.g., $\mathcal{O}(1)$ $\mu$K$^2$). Therefore Planck's angular power spectra alone are not sufficient to establish a preference for lower values of the $u$ ratio. However the suppression of power that such values ($u = 10^{-3}$ and $u = 10^{-4}$) induce in the matter power spectrum are very different. Using the $\sigma_8$ value together with the angular power spectra, we can rule out $u = 10^{-3}$.

## III. METHOD

The Boltzmann equations in presence of dark matter-neutrino interactions were given in e.g., Ref. [13,14]. To ensure the full treatment of the Boltzmann hierarchy, we use a modified version of the Boltzmann code CLASS[1] [25,26], that incorporates the dark matter-neutrino interactions [21]. The constraints are derived using the Markov Chain Monte Carlo tool Monte Python [27], interfaced with our version of CLASS, that fully supports the Planck data release 2015 Likelihood Code [24].

We perform our analysis in three main steps.

In our first analysis, we use the six cosmological parameters of the standard model (namely the baryonic density $\Omega_b h^2$, the dark matter density $\Omega_c h^2$, the ratio between the sound horizon and the angular diameter distance at decoupling $\Theta_s$, the reionization optical depth $\tau$, the spectral index of the scalar perturbations $n_S$, the amplitude of the primordial power spectrum $A_S$) plus the ratio $u \equiv u_\nu = \sigma_{DM-\nu}/m_{DM}$.

In a second step, we consider eight free parameters, i.e., the seven parameters mentioned above + either the effective number of relativistic degrees of freedom $N_{eff}$ or the total neutrino mass $\Sigma m_\nu$. Our rationale for doing this is that adding a dark radiation component ($N_{eff} > 3.046$ [28]) as in Ref. [21,29,30] or allowing the sum of the neutrino masses $\Sigma m_\nu$ to depart from the benchmark value taken by the Planck collaboration ($\Sigma m_\nu = 0.06$ eV) could reduce current tensions on the age of the Universe.

Our last analysis uses nine free parameters, namely the seven mentioned above $+ N_{eff} + \Sigma m_\nu$. Note that we use a logarithmic prior to constrain the $u$ parameter and flat priors for the other parameters (i.e., $\Omega_b h^2$, $\Omega_c h^2$, $\Theta_s$, $\tau$, $n_S$, $A_S$, $N_{eff}$, and $\Sigma m_\nu$[2]).

To understand the impact of the polarization data, we start by analysing the full range of the 2015 temperature power spectrum ($2 \leq \ell \leq 2500$) plus the low multipoles polarization data ($2 \leq \ell \leq 29$) [24]. We will refer to this analysis as the "Planck TT + lowTEB" data sets. We then perform a second analysis, which we will refer to as "Planck TTTEEE + lowTEB," where we include the Planck high multipole polarization data [24]. Finally, we perform a third analysis where we include the 2015 Planck measurements of the CMB lensing potential power spectrum $C_\ell^{\phi\phi}$ [35]. This last analysis will be referred to as the "lensing" data set.

The scenarios for which the $H_0$ tension between the model-dependent Planck value and that inferred from the observations of Cepheids variables [23] appears to be less than $2\sigma$ are analysed again. This time, we assume a Gaussian prior on $H_0$ (i.e., $H_0 = 73.24 \pm 1.75$ km s$^{-1}$ Mpc$^{-1}$) and refer to this set of analysis as "R16".

## IV. RESULTS BASED ON THE "PLANCK TT + LOWTEB" DATASETS ONLY

We now present the results of our analyses using the Planck low multipole polarization data. The 68% confidence level (C.L.) limits on the cosmological parameters for the DM-$\nu$ scenario are shown in Table I. For comparison, we also display the 68% C.L. constraints obtained by the Planck collaboration [36] for collisionless LCDM[3] in Table II.

"Weak" interactions are expected to erase primordial scales which have not been observed yet. Hence our analysis is bound to exclude only the strongest DM-$\nu$ interactions. This translates into an upper bound on the $u$ parameter of $u < 10^{-4.1}$ (or $u < 10^{-4.0}$, using the lensing data sets), corresponding to a DM-$\nu$ elastic cross section of $\sigma \simeq 3–6 \times 10^{-31}$ $(m_{dm}/\text{GeV})$ cm$^2$. This result is similar to the limit derived in Ref. [37], using the 2013 Planck temperature data. Furthermore, we find that the Planck data prefer low values of the Hubble constant $H_0$, even in the presence of DM-$\nu$ interactions (see Table. I). This is at odds with the conclusions from Ref. [16] but a possible explanation is that the inclusion of the $\sigma_8$ constraint and the

[1]class-code.net.

[2]There is no consensus yet on the prior that should be used to constrain the total neutrino mass $\Sigma m_\nu$ using CMB data (see for example [31–34]). Here we use a flat prior for our analysis to be as much conservative as possible.

[3]https://wiki.cosmos.esa.int/planckpla2015/images/f/f7/Baseline_params_table_2015_limit68.pdf.

TABLE I. 68% C.L. constraints on cosmological parameters with interactions, for the Planck TT + lowTEB and the Planck TT + lowTEB + lensing combination of datasets. When only upper limits are shown, they correspond to 95% C.L. limits.

| $\Lambda$CDM + $u$ | | | $+N_{\rm eff}$ | $+N_{\rm eff}$ | $+\Sigma m_\nu$ | $+\Sigma m_\nu$ | $+N_{\rm eff}+\Sigma m_\nu$ | $+N_{\rm eff}+\Sigma m_\nu$ |
|---|---|---|---|---|---|---|---|---|
| Parameter | Planck TT+ lowTEB | Planck TT+ lowTEB + lensing | Planck TT+ lowTEB | Planck TT+ lowTEB + lensing | Planck TT+ lowTEB | Planck TT+ lowTEB + lensing | Planck TT+ lowTEB | Planck TT+ lowTEB + lensing |
| $\Omega_b h^2$ | $0.02224^{+0.00023}_{-0.00024}$ | $0.02226^{+0.00027}_{-0.00026}$ | $0.02232^{+0.00037}_{-0.00041}$ | $0.02234^{+0.00035}_{-0.00040}$ | $0.02214^{+0.00027}_{-0.00026}$ | $0.02217 \pm 0.00029$ | $0.02219^{+0.00043}_{-0.00044}$ | $0.02224^{+0.00037}_{-0.00042}$ |
| $\Omega_c h^2$ | $0.1195^{+0.0022}_{-0.0023}$ | $0.1186^{+0.0021}_{-0.0022}$ | $0.1205^{+0.0039}_{-0.0045}$ | $0.1197^{+0.0039}_{-0.0041}$ | $0.1200^{+0.0025}_{-0.0026}$ | $0.1195^{+0.0024}_{-0.0025}$ | $0.1206 \pm 0.0046$ | $0.1206^{+0.0038}_{-0.0041}$ |
| $\tau$ | $0.079^{+0.018}_{-0.020}$ | $0.070^{+0.015}_{-0.018}$ | $0.083^{+0.018}_{-0.024}$ | $0.074^{+0.016}_{-0.021}$ | $0.080^{+0.018}_{-0.020}$ | $0.074^{+0.018}_{-0.019}$ | $0.083^{+0.021}_{-0.024}$ | $0.077^{+0.017}_{-0.022}$ |
| $n_s$ | $0.9652^{+0.0066}_{-0.0065}$ | $0.9667^{+0.0071}_{-0.0065}$ | $0.969^{+0.015}_{-0.017}$ | $0.971^{+0.014}_{-0.017}$ | $0.9623^{+0.0083}_{-0.0082}$ | $0.9640^{+0.0077}_{-0.0083}$ | $0.965 \pm 0.018$ | $0.968^{+0.015}_{-0.017}$ |
| $\ln(10^{10}A_s)$ | $3.091^{+0.034}_{-0.039}$ | $3.071^{+0.027}_{-0.033}$ | $3.100^{+0.040}_{-0.053}$ | $3.080^{+0.034}_{-0.044}$ | $3.094^{+0.035}_{-0.039}$ | $3.080^{+0.033}_{-0.034}$ | $3.101^{+0.042}_{-0.054}$ | $3.089^{+0.036}_{-0.046}$ |
| $H_0$ [Km s$^{-1}$ Mpc$^{-1}$] | $67.5 \pm 1.0$ | $67.8 \pm 1.0$ | $68.3^{+2.6}_{-3.2}$ | $68.7^{+2.4}_{-3.0}$ | $65.7^{+2.6}_{-1.9}$ | $66.2^{+2.2}_{-1.9}$ | $66.2^{+4.0}_{-3.7}$ | $67.0^{+3.3}_{-3.5}$ |
| $\sigma_8$ | $0.825^{+0.017}_{-0.016}$ | $0.814^{+0.014}_{-0.012}$ | $0.830^{+0.021}_{-0.025}$ | $0.819^{+0.019}_{-0.021}$ | $0.788^{+0.054}_{-0.033}$ | $0.787^{+0.036}_{-0.030}$ | $0.792^{+0.060}_{-0.040}$ | $0.791^{+0.041}_{-0.031}$ |
| $\mathrm{Log}(u)$ | $< -4.1$ | $< -4.0$ | $< -4.0$ | $< -4.0$ | $< -4.0$ | $< -4.1$ | $< -4.0$ | $< -4.0$ |
| $N_{\rm eff}$ | 3.046 | 3.046 | $3.14^{+0.32}_{-0.35}$ | $3.15^{+0.28}_{-0.33}$ | 3.046 | 3.046 | $3.10 \pm 0.35$ | $3.14^{+0.30}_{-0.33}$ |
| $\Sigma m_\nu$ [eV] | 0.06 | 0.06 | 0.06 | 0.06 | $< 2.0$ | $<1.6$ | $<2.2$ | $<1.6$ |

TABLE II. 68% C.L. constraints on cosmological parameters without interactions, for the Planck TT + lowTEB and the Planck TT + lowTEB + lensing combination of data sets. When only upper limits are shown, they correspond to 95% C.L. limits.

| $\Lambda$CDM | | | $+N_{\rm eff}$ | $+N_{\rm eff}$ | $+\Sigma m_\nu$ | $+\Sigma m_\nu$ | $+N_{\rm eff}+\Sigma m_\nu$ | $+N_{\rm eff}+\Sigma m_\nu$ |
|---|---|---|---|---|---|---|---|---|
| Parameter | Planck TT+ lowTEB | Planck TT+ lowTEB + lensing | Planck TT+ lowTEB | Planck TT+ lowTEB + lensing | Planck TT+ lowTEB | Planck TT+ lowTEB + lensing | Planck TT+ lowTEB | Planck TT+ lowTEB + lensing |
| $\Omega_b h^2$ | $0.02222 \pm 0.00023$ | $0.02226 \pm 0.00023$ | $0.02230 \pm 0.00037$ | $0.02232^{+0.00035}_{-0.00039}$ | $0.02213 \pm 0.00027$ | $0.02211 \pm 0.00026$ | $0.02215 \pm 0.00041$ | $0.02212 \pm 0.00041$ |
| $\Omega_c h^2$ | $0.1197 \pm 0.0022$ | $0.1186 \pm 0.0020$ | $0.1205 \pm 0.0041$ | $0.1195^{+0.0037}_{-0.0043}$ | $0.1202 \pm 0.0024$ | $0.1199^{+0.0023}_{-0.0026}$ | $0.1205 \pm 0.0039$ | $0.1201 \pm 0.0039$ |
| $\tau$ | $0.078 \pm 0.019$ | $0.066 \pm 0.016$ | $0.080 \pm 0.022$ | $0.069 \pm 0.020$ | $0.080 \pm 0.020$ | $0.075 \pm 0.018$ | $0.081 \pm 0.021$ | $0.076 \pm 0.20$ |
| $n_s$ | $0.9655 \pm 0.0062$ | $0.9677 \pm 0.0060$ | $0.969 \pm 0.016$ | $0.971 \pm 0.015$ | $0.9637 \pm 0.0071$ | $0.9640 \pm 0.0068$ | $0.965 \pm 0.016$ | $0.965 \pm 0.016$ |
| $\ln(10^{10}A_s)$ | $3.089 \pm 0.036$ | $3.062 \pm 0.029$ | $3.096 \pm 0.047$ | $3.070 \pm 0.042$ | $3.095 \pm 0.038$ | $3.083 \pm 0.035$ | $3.098 \pm 0.046$ | $3.085 \pm 0.044$ |
| $H_0$ [Km s$^{-1}$ Mpc$^{-1}$] | $67.31 \pm 0.96$ | $67.81 \pm 0.92$ | $68.0^{+2.6}_{-3.0}$ | $68.5^{+2.5}_{-3.0}$ | $65.6^{+3.1}_{-1.4}$ | $65.2^{+3.2}_{-2.0}$ | $65.8^{+4.5}_{-3.3}$ | $65.3^{+4.2}_{-3.8}$ |
| $\sigma_8$ | $0.829 \pm 0.014$ | $0.8149 \pm 0.0093$ | $0.834^{+0.022}_{-0.025}$ | $0.820^{+0.018}_{-0.021}$ | $0.796^{+0.057}_{-0.023}$ | $0.776^{+0.047}_{-0.025}$ | $0.796^{+0.065}_{-0.030}$ | $0.777^{+0.052}_{-0.035}$ |
| $N_{\rm eff}$ | 3.046 | 3.046 | $3.13^{+0.30}_{-0.34}$ | $3.13^{+0.29}_{-0.34}$ | 3.046 | 3.046 | $3.08 \pm 0.31$ | $3.07 \pm 0.31$ |
| $\Sigma m_\nu$ [eV] | 0.06 | 0.06 | 0.06 | 0.06 | $<0.715$ | $<0.675$ | $<0.725$ | $<0.677$ |

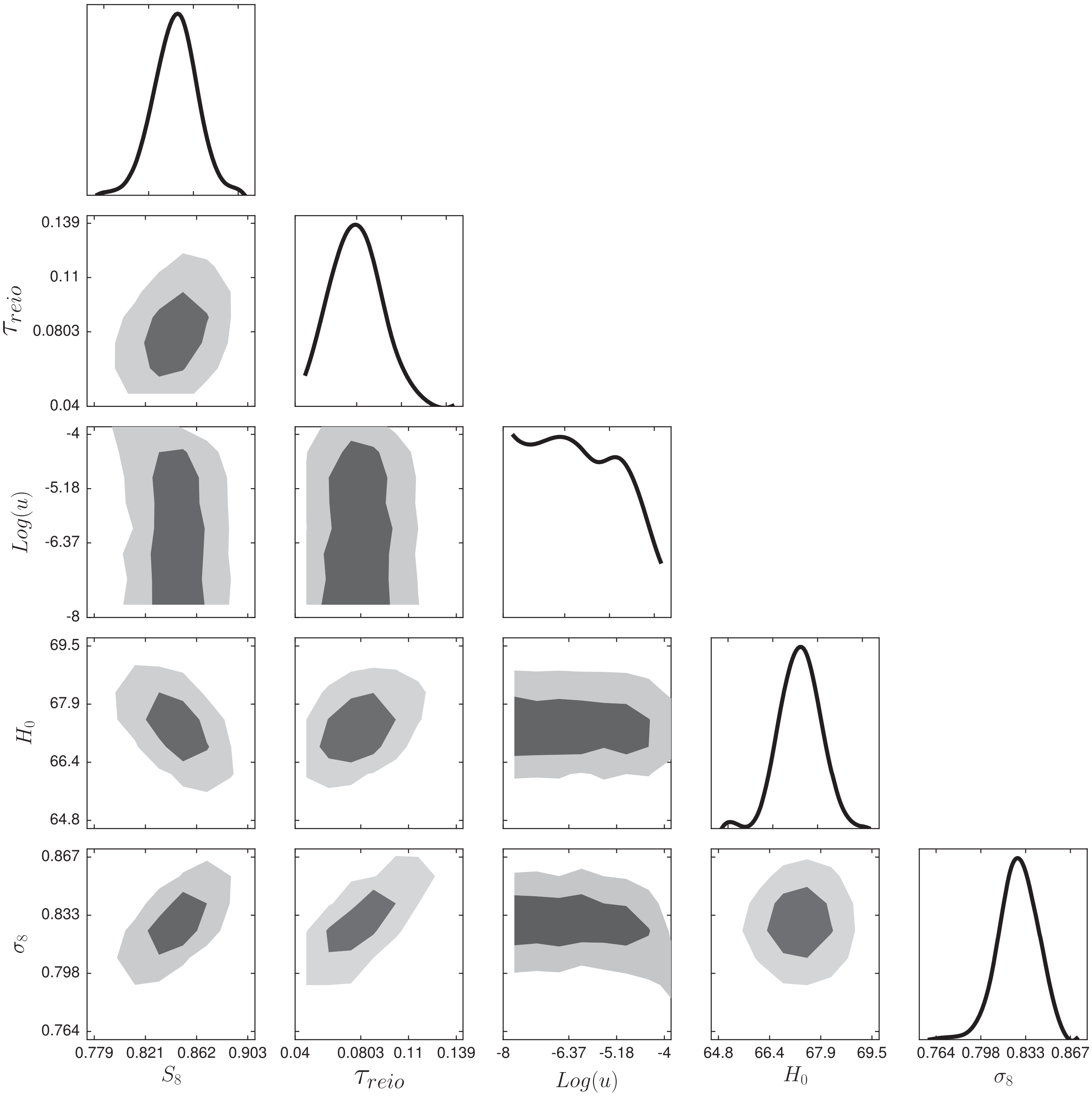


FIG. 3. Triangle plot showing the 1D and 2D posterior distributions of the cosmological parameters for Planck TT + lowTEB in the $\Lambda\mathrm{CDM} + u + N_{\mathrm{eff}}$ scenario.

use of the low-$l$ Planck's polarization data instead of the WMAP polarization data, can lead to new results.

We observe in addition that the introduction of the DM-$\nu$ interactions breaks the well-known degeneracy between $H_0$ and the clustering parameter $\sigma_8$. The Hubble constant slightly increases (by about $0.2\sigma$) while the clustering parameter $\sigma_8$ slightly decreases (by about $0.3\sigma$) in presence of such interactions. For example, we find $\sigma_8 = 0.825^{+0.017}_{-0.016}$ (see the first column of the Table I) while the Planck collaboration found $\sigma_8 = 0.829 \pm 0.014$ using the same dataset combination (see the first column of the Table II) for collisionless LCDM.

When we allow $N_{\mathrm{eff}}$ to vary, we obtain $N_{\mathrm{eff}} = 3.14^{+0.32}_{-0.35}$ for $\Sigma m_\nu = 0.06$ eV (see the third column of the Table I and Fig. 3). This result is a bit higher than the standard model value ($N_{\mathrm{eff}} = 3.046$) but it does remain compatible with it nonetheless. The Hubble rate then shifts by about $0.1\sigma$ from $H_0 = 68.0^{+2.6}_{-3.0}\,\mathrm{km\,s^{-1}\,Mpc^{-1}}$ to $H_0 = 68.3^{+2.6}_{-3.2}\,\mathrm{km\,s^{-1}\,Mpc^{-1}}$ (see the third columns of Table II and Table I respectively). In this case, the tension between the local measurements of

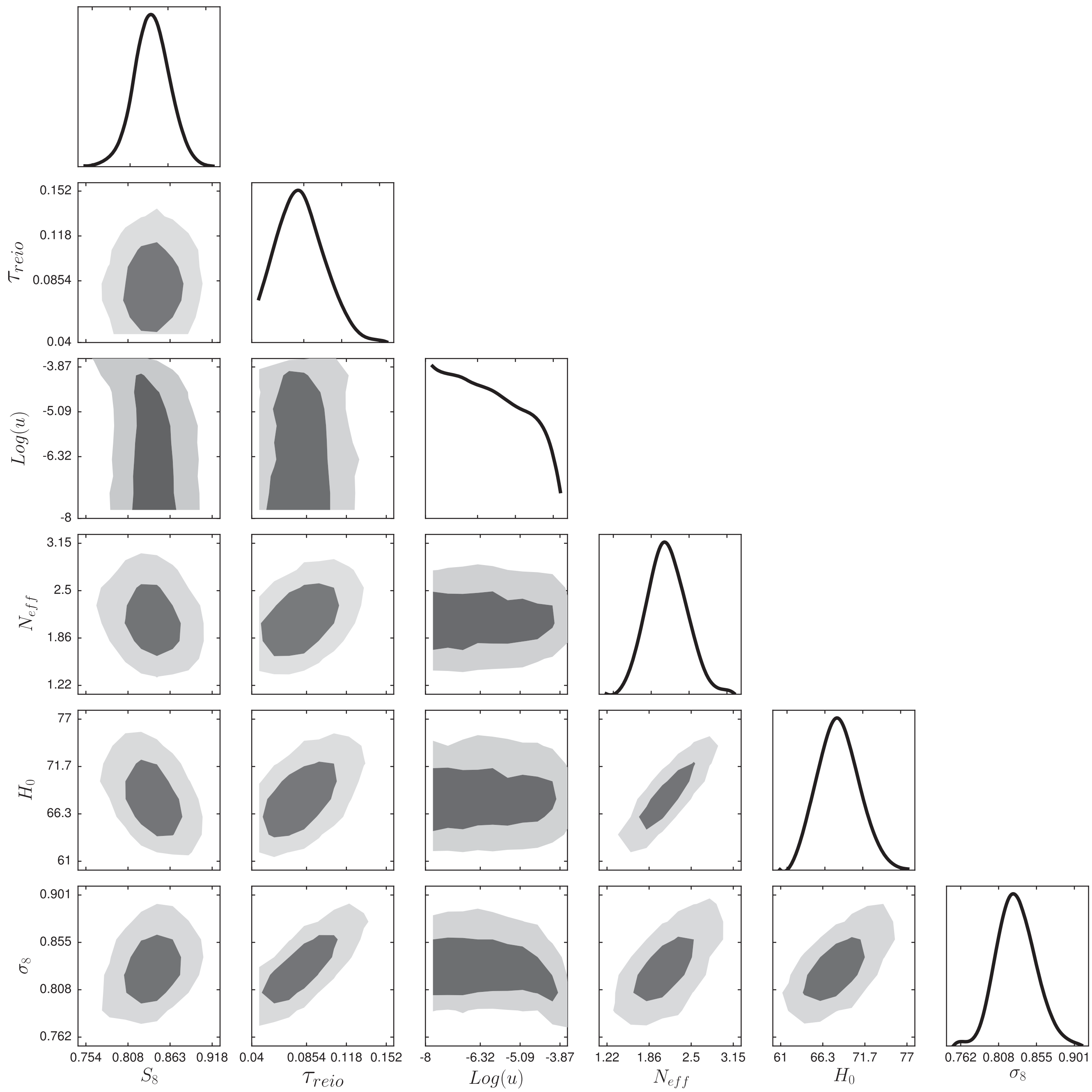


FIG. 4. Triangle plot showing the 1D and 2D posterior distributions of the cosmological parameters for Planck TT + lowTEB in the $\Lambda$CDM + $u$ + $\Sigma m_\nu$ scenario.

$H_0$ ($H_0 = 73.24 \pm 1.75\ \mathrm{km\,s^{-1}\,Mpc^{-1}}$) [23], and the Planck $\Lambda$CDM value [36] is somewhat reduced. Therefore we can reasonably combine the Planck data sets with the R16 data sets and perform a new analysis. The results are given in Table V. A positive correlation between $H_0$ and $\sigma_8$ also exists when $N_{\rm eff}$ is free to vary while we find a negative correlation between $S_8 \equiv \sigma_8\sqrt{\Omega_m/0.3}$ (the quantity that is measured by the weak lensing experiment) and $H_0$, as can be seen in Fig. 3 where $S_8 = 0.840 \pm 0.027$. For this reason if we add the R16 dataset, that prefers a higher value for the Hubble constant, we have a shift towards lower values of $S_8 = 0.825^{+0.026}_{-0.022}$ of about $0.6\sigma$. Hence, in a $\Lambda$CDM + $u$ + $N_{\rm eff}$ scenario, for Planck TT + lowTEB + R16 data sets combination, also the tension with the KiDS-450 measurements ($S_8 = 0.745 \pm 0.039$ [38]) is reduced to about $1.8\sigma$.

The introduction of DM-$\nu$ interactions is also compatible with heavier neutrinos. This is an important point since it was noted in Refs. [30,39,40] that massive neutrinos could alleviate the tension between Planck and the weak lensing measurements from the CFHTLenS survey [41,42] and

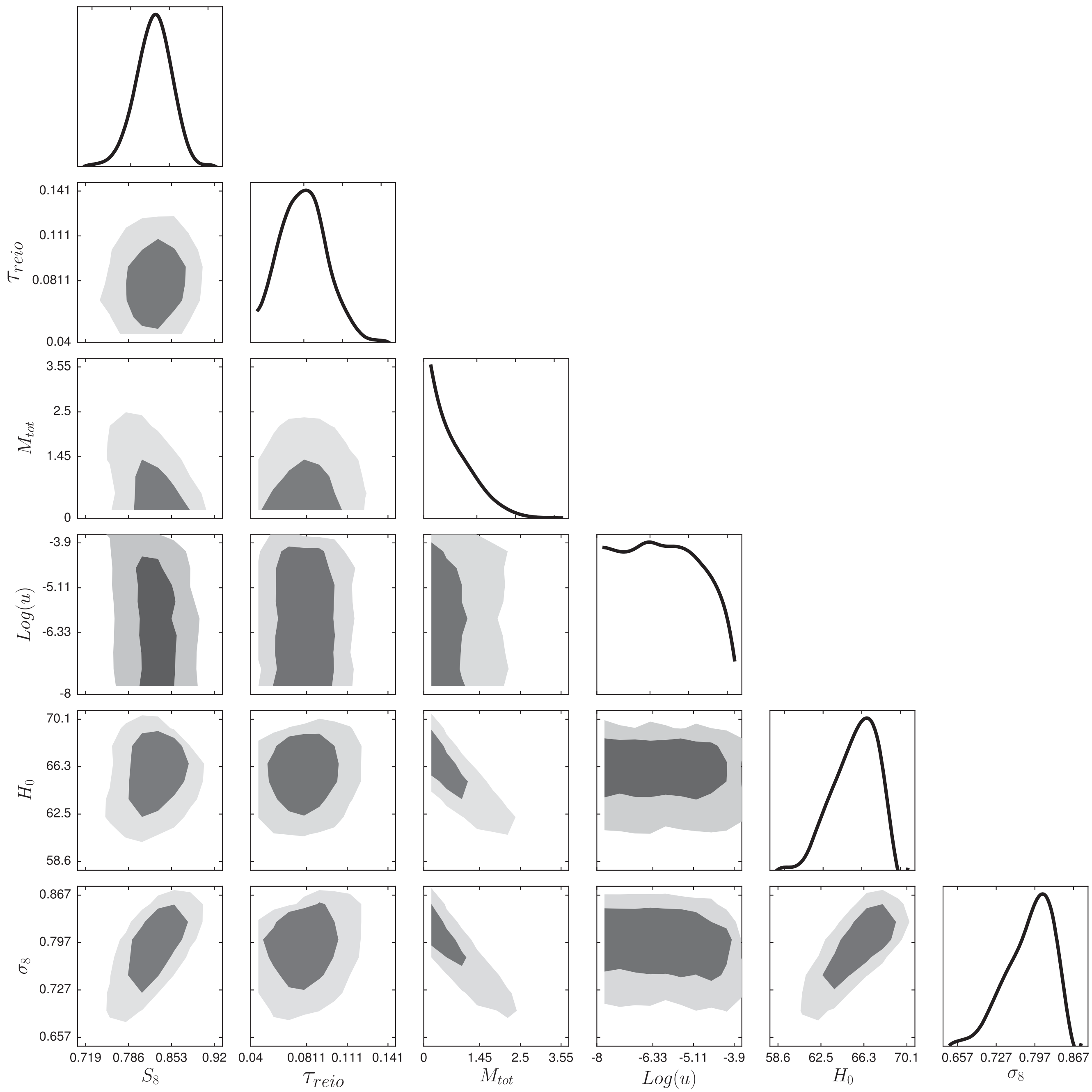


FIG. 5. Triangle plot showing the 1D and 2D posterior distributions of the cosmological parameters for Planck TT + lowTEB in the $\Lambda\text{CDM} + u + N_{\text{eff}} + \Sigma m_\nu$ scenario.

KiDS-450 [38]. Assuming DM-$\nu$ interactions and the Planck TT + lowTEB + lensing data set, we obtain $\Sigma m_\nu < 1.6$ eV at 95% C.L. (see the sixth column of Table I) instead of $\Sigma m_\nu < 0.675$ eV for LCDM (see the sixth column of Table II).

For that same combination of data sets (Planck TT+ lowTEB + lensing), both the Hubble constant $H_0$ and the clustering parameter $\sigma_8$ increase with respect to the standard model ($\Lambda\text{CDM} + \Sigma m_\nu$) value, by about $0.5\sigma$ and $0.4\sigma$ respectively. However, the value of $\sigma_8$ thus obtained remains small enough to partially reduce the tension with the weak lensing measurements. We obtain $\sigma_8 = 0.787^{+0.036}_{-0.030}$ which is much lower than the Planck value $\sigma_8 = 0.8149 \pm 0.0093$, which was reported by the collaboration for LCDM only (i.e., LCDM + fixed values of $N_{\text{eff}}$ and $\Sigma m_\nu$) using the Planck TT + lowTEB + lensing data set. Even though the tension between $H_0$ and $\sigma_8$ is restored in this scenario, the Hubble constant remains uncorrelated with $S_8$, as we can see in Fig. 4. Indeed, using the Planck

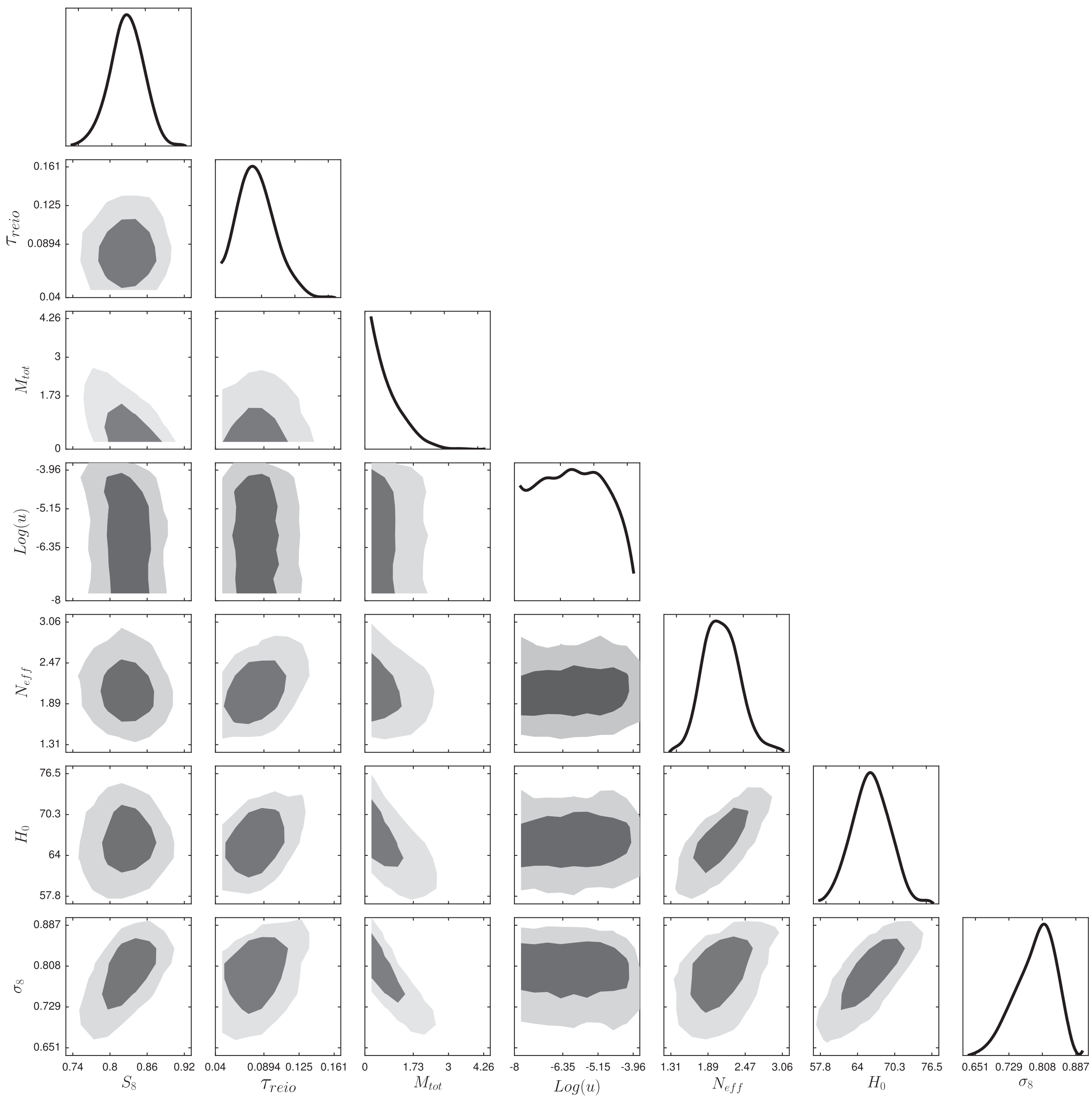


FIG. 6. Triangle plot showing the 1D and 2D posterior distributions of the cosmological parameters for Planck TTTEEE + lowTEB in the $\Lambda$CDM + $u$ scenario.

TT + lowTEB data set only, we find $S_8 = 0.826^{+0.033}_{-0.028}$. Therefore adding the DM-$\nu$ interactions does reduce the tension with the KiDS-450 measurements to about $1.7\sigma$.

Finally, the tension between $H_0$ and $\sigma_8$ can be reduced by varying $N_{\rm eff}$ and $\Sigma m_\nu$ simultaneously. Using the Planck TT + lowTEB data sets, we find $H_0 = 66.2^{+4.0}_{-3.7}$ and $\sigma_8 = 0.792^{+0.060}_{-0.040}$, as shown in the seventh column of the Table I and in Fig. 5, which represents a $0.1\sigma$ shift for $H_0$ and $-0.1\sigma$ shift for $\sigma_8$ with respect to LCDM.

The tension with other $H_0$ measurements is then about $1.6\sigma$. The new value for $S_8$ (namely $S_8 = 0.826^{+0.033}_{-0.027}$), that is not correlated with $H_0$ as we can see in Fig. 5, also reduces the tension with KiDS-450 [38] to about $1.7\sigma$.

## V. RESULTS WITH THE POLARIZATION DATA

In Table III, we report the 68% C.L. limits on the DM-$\nu$ scenario obtained using the polarization data. For

TABLE III. 68% C.L. constraints on cosmological parameters with interactions, for the Planck TTTEEE + lowTEB and the Planck TTTEEE + lowTEB + lensing combination of data sets. When only upper limits are shown, they correspond to 95% C.L. limits.

| $\Lambda$CDM + $u$ | | | $+N_{\rm eff}$ | $+N_{\rm eff}$ | $+\Sigma m_\nu$ | $+\Sigma m_\nu$ | $+N_{\rm eff}+\Sigma m_\nu$ | $+N_{\rm eff}+\Sigma m_\nu$ |
|---|---|---|---|---|---|---|---|---|
| Parameter | Planck TTTEEE+ lowTEB | Planck TTTEEE+ lowTEB + lensing | Planck TTTEEE+ lowTEB | Planck TTTEEE+ lowTEB + lensing | Planck TTTEEE+ lowTEB | Planck TTTEEE+ lowTEB + lensing | Planck TTTEEE+ lowTEB | Planck TTTEEE+ lowTEB + lensing |
| $\Omega_b h^2$ | $0.02225 \pm 0.00017$ | $0.02225,^{+0.00017}_{-0.00018}$ | $0.02218 \pm 0.00028$ | $0.02216^{+0.00023}_{-0.00025}$ | $0.02219^{+0.00018}_{-0.00017}$ | $0.02219 \pm 0.00018$ | $0.02212^{+0.00029}_{-0.00031}$ | $0.02210^{+0.00025}_{-0.00026}$ |
| $\Omega_c h^2$ | $0.1198^{+0.0016}_{-0.0015}$ | $0.1194 \pm 0.0015$ | $0.1190^{+0.0035}_{-0.0036}$ | $0.1179 \pm 0.0030$ | $0.1200 \pm 0.0016$ | $0.1197^{+0.0015}_{-0.0016}$ | $0.1188^{+0.0038}_{-0.0037}$ | $0.1185 \pm 0.0032$ |
| $\tau$ | $0.080^{+0.016}_{-0.018}$ | $0.066^{+0.013}_{-0.015}$ | $0.078^{+0.018}_{-0.019}$ | $0.065^{+0.011}_{-0.015}$ | $0.082^{+0.018}_{-0.017}$ | $0.073^{+0.015}_{-0.016}$ | $0.080^{+0.019}_{-0.021}$ | $0.071^{+0.014}_{-0.016}$ |
| $n_s$ | $0.9639^{+0.0053}_{-0.0052}$ | $0.9644^{+0.0056}_{-0.0054}$ | $0.961 \pm 0.011$ | $0.9603^{+0.0093}_{-0.0095}$ | $0.9620^{+0.0060}_{-0.0056}$ | $0.9628^{+0.0057}_{-0.0055}$ | $0.959^{+0.012}_{-0.013}$ | $0.959 \pm 0.010$ |
| $\ln(10^{10}A_s)$ | $3.093^{+0.032}_{-0.035}$ | $3.065^{+0.024}_{-0.027}$ | $3.087^{+0.040}_{-0.041}$ | $3.059^{+0.024}_{-0.030}$ | $3.099^{+0.035}_{-0.033}$ | $3.079^{+0.028}_{-0.031}$ | $3.092^{+0.041}_{-0.043}$ | $3.072^{+0.030}_{-0.034}$ |
| $H_0$ [Km s$^{-1}$ Mpc$^{-1}$] | $67.32^{+0.70}_{-0.71}$ | $67.50^{+0.70}_{-0.71}$ | $66.8^{+1.8}_{-1.9}$ | $66.8 \pm 1.6$ | $66.0^{+2.3}_{-1.2}$ | $66.1^{+1.9}_{-1.3}$ | $65.4^{+2.8}_{-2.5}$ | $65.4^{+2.2}_{-2.0}$ |
| $\sigma_8$ | $0.827^{+0.016}_{-0.015}$ | $0.814^{+0.013}_{-0.012}$ | $0.822 \pm 0.023$ | $0.809^{+0.013}_{-0.014}$ | $0.797^{+0.049}_{-0.023}$ | $0.789^{+0.036}_{-0.020}$ | $0.791^{+0.052}_{-0.050}$ | $0.784^{+0.035}_{-0.024}$ |
| Log($u$) | $< -4.1$ | $< -4.1$ | $< -4.0$ | $< -4.0$ | $< -4.1$ | $< -4.2$ | $< -3.9$ | $< -4.3$ |
| $N_{\rm eff}$ | 3.046 | 3.046 | $2.98^{+0.23}_{-0.24}$ | $2.94 \pm 0.20$ | 3.046 | 3.046 | $2.96^{+0.23}_{-0.28}$ | $2.95^{+0.20}_{-0.21}$ |
| $\Sigma m_\nu$ [eV] | 0.06 | 0.06 | 0.06 | 0.06 | $< 1.9$ | $< 1.5$ | $< 2.0$ | $< 1.6$ |

TABLE IV. 68% C.L. constraints on cosmological parameters without interactions, for the Planck TTTEEE + lowTEB and the Planck TTTEEE + lowTEB + lensing combination of data sets. When only upper limits are shown, they correspond to 95% C.L. limits.

| $\Lambda$CDM | | | $+N_{\rm eff}$ | $+N_{\rm eff}$ | $+\Sigma m_\nu$ | $+\Sigma m_\nu$ | $+N_{\rm eff}+\Sigma m_\nu$ | $+N_{\rm eff}+\Sigma m_\nu$ |
|---|---|---|---|---|---|---|---|---|
| Parameter | Planck TTTEEE+ lowTEB | Planck TTTEEE+ lowTEB + lensing | Planck TTTEEE +lowTEB | Planck TTTEEE+ lowTEB + lensing | Planck TTTEEE +lowTEB | Planck TTTEEE+ lowTEB + lensing | Planck TTTEEE +lowTEB | Planck TTTEEE+ lowTEB + lensing |
| $\Omega_b h^2$ | $0.02225 \pm 0.00016$ | $0.02226 \pm 0.00016$ | $0.02220 \pm 0.00024$ | $0.02216 \pm 0.00023$ | $0.02222 \pm 0.00017$ | $0.02219 \pm 0.00017$ | $0.02215 \pm 0.00025$ | $0.02208 \pm 0.000025$ |
| $\Omega_c h^2$ | $0.1198 \pm 0.0015$ | $0.1193 \pm 0.0014$ | $0.1191 \pm 0.0031$ | $0.1178 \pm 0.0030$ | $0.1200 \pm 0.0015$ | $0.1198 \pm 0.0015$ | $0.1191 \pm 0.0031$ | $0.1184 \pm 0.0030$ |
| $\tau$ | $0.079 \pm 0.017$ | $0.063 \pm 0.014$ | $0.077 \pm 0.0018$ | $0.060 \pm 0.014$ | $0.083 \pm 0.018$ | $0.074 \pm 0.017$ | $0.081 \pm 0.018$ | $0.071 \pm 0.018$ |
| $n_s$ | $0.9645 \pm 0.0049$ | $0.9653 \pm 0.0048$ | $0.9620 \pm 0.0097$ | $0.9606 \pm 0.0092$ | $0.9639 \pm 0.0050$ | $0.9637 \pm 0.0051$ | $0.9610 \pm 0.0099$ | $0.9589 \pm 0.0095$ |
| $\ln(10^{10}A_s)$ | $3.094 \pm 0.034$ | $3.059 \pm 0.025$ | $3.088 \pm 0.038$ | $3.049 \pm 0.029$ | $3.100 \pm 0.034$ | $3.081 \pm 0.033$ | $3.095 \pm 0.039$ | $3.071 \pm 0.037$ |
| $H_0$ [Km s$^{-1}$ Mpc$^{-1}$] | $67.27 \pm 0.66$ | $67.51 \pm 0.64$ | $66.8 \pm 1.6$ | $66.7 \pm 1.5$ | $66.3^{+2.0}_{-0.9}$ | $65.6^{+2.5}_{-1.4}$ | $65.8^{+2.6}_{-1.8}$ | $64.8^{+2.5}_{-2.1}$ |
| $\sigma_8$ | $0.831 \pm 0.013$ | $0.8150 \pm 0.0087$ | $0.828 \pm 0.018$ | $0.809 \pm 0.013$ | $0.812^{+0.039}_{-0.017}$ | $0.783^{+0.040}_{-0.020}$ | $0.807^{+0.022}_{-0.044}$ | $0.778^{+0.038}_{-0.024}$ |
| $N_{\rm eff}$ | 3.046 | 3.046 | $2.99 \pm 0.20$ | $2.94 \pm 0.20$ | 3.046 | 3.046 | $2.98 \pm 0.20$ | $2.93 \pm 0.19$ |
| $\Sigma m_\nu$ [eV] | 0.06 | 0.06 | 0.06 | 0.06 | $< 0.492$ | $< 0.589$ | $< 0.494$ | $< 0.577$ |

comparison, we also give the 68% C.L. limits[4] obtained by the Planck collaboration [36] for the LCDM scenario in Table IV.

Assuming fixed values of $N_{\rm eff}$ and $\Sigma m_\nu$, we find that the use of the Planck polarization data generally slightly improves the constraints of the strength of the dark matter-neutrino interactions (see Fig. 6). For example, instead of $u < 10^{-4.0}$, we now find $u < 10^{-4.3}$ using the Planck TTTEEE + lowTEB + lensing data sets and the scenario with nine parameters (see last column of Table III). The rest of the parameters remain compatible with ΛCDM values.

Similarly to the analysis performed in Sec. IV, we also vary the effective number of relativistic degrees of freedom $N_{\rm eff}$. However it remains consistent with the standard model value, and so does the Hubble constant $H_0$ in this case (see, for example, the third column of the Tables III and IV).

Adding the polarization data however helps to relax the bounds on massive neutrinos. The latter shifts from $\Sigma m_\nu < 0.492$ eV for the Planck TTTEEE + lowTEB data sets without interactions to $\Sigma m_\nu < 1.9$ eV for the same combination of data sets in presence of interactions (see the fifth column of Table IV and Table III, respectively). Furthermore, $\sigma_8$ decreases a bit in presence of interactions. We find $\sigma_8 = 0.797^{+0.049}_{-0.023}$ in presence of interactions versus $\sigma_8 = 0.812^{+0.039}_{-0.017}$ in ΛCDM, i.e., $0.9\sigma$ lower, as shown in the fifth column of Tables III and IV. Here again, we find that the tension with the weak lensing measurements is reduced. We obtain $S_8 = 0.832^{+0.029}_{-0.022}$ in presence of interactions (and letting $\Sigma m_\nu$ free to vary) for the Planck TTTEEE + lowTEB data sets, which decreases the tension with KiDS-450 to $1.8\sigma$. An opposite trend is present if we add the lensing data set. In fact we find $\sigma_8 = 0.789^{+0.036}_{-0.020}$ in presence of interactions versus $\sigma_8 = 0.783^{+0.040}_{-0.020}$ in ΛCDM, i.e., $0.2\sigma$ higher, as shown in the six column of Tables III and IV.

Finally, we observe a small shift in both values of $H_0$ and $\sigma_8$ with respect to ΛCDM when we vary $N_{\rm eff}$ and $\Sigma m_\nu$ both simultaneously. The upper bound on $\Sigma m_\nu$ is also relaxed with respect to the collisionless ΛCDM. Adding the lensing dataset, we obtain for example $H_0 = 65.4^{+2.2}_{-2.0}$ and $\sigma_8 = 0.784^{+0.035}_{-0.024}$, i.e., a shift of $0.2\sigma$ for both, while we have $S_8 = 0.820^{+0.019}_{-0.015}$, as shown in the eight column of the Table III. Whilst the new value of $H_0$ does not remove completely the tensions between the different observation data sets, it does reduce the $S_8$ tension to $1.7\sigma$.

We note that when the dark matter-neutrino interactions are introduced, the scalar spectral index ($n_S$) gets very slightly shifted towards smaller values (few fractions of $\sigma$), for most of the data set combinations and parameters considered in this paper. This shift is due to the fact that the interactions change all the acoustic peaks (see Fig. 1 and discussion in Sec. II). In fact, they increase the low multipoles due to the suppression of neutrino free-streaming and decrease the high multipoles due to the collisional damping. Therefore, in order to reconcile the prediction of this model with the observed angular power spectra, the increase in the Hubble constant needs to be compensated by a change in the spectrum tilt.

[4]https://wiki.cosmos.esa.int/planckpla2015/images/f/f7/Baseline_params_table_2015_limit68.pdf.

TABLE V. 68% C.L. constraints on cosmological parameters with interactions, for the Planck TT + lowTEB + R16 combination of datasets. If only upper limits are shown, they are at 95% C.L.

| ΛCDM + $u$ | $+N_{\rm eff}$ | $+N_{\rm eff} + \Sigma m_\nu$ |
|---|---|---|
| Parameter | Planck TT + lowTEB + R16 | Planck TT + lowTEB + R16 |
| $\Omega_b h^2$ | $0.02278^{+0.00026}_{-0.00025}$ | $0.02278 \pm 0.00027$ |
| $\Omega_c h^2$ | $0.1238^{+0.0037}_{-0.0038}$ | $0.1240^{+0.0035}_{-0.0045}$ |
| $\tau$ | $0.099^{+0.019}_{-0.021}$ | $0.100^{+0.023}_{-0.021}$ |
| $n_s$ | $0.9898^{+0.0088}_{-0.0094}$ | $0.990^{+0.009}_{-0.010}$ |
| $\ln(10^{10}A_s)$ | $3.143^{+0.041}_{-0.039}$ | $3.145^{+0.054}_{-0.037}$ |
| $H_0$ [Km s$^{-1}$ Mpc$^{-1}$] | $72.1^{+1.5}_{-1.7}$ | $71.9^{+1.6}_{-1.8}$ |
| $\sigma_8$ | $0.850^{+0.024}_{-0.018}$ | $0.846^{+0.030}_{-0.025}$ |
| Log($u$) | $< -4.0$ | $< -4.0$ |
| $N_{\rm eff}$ | 3.54, ±0.20 | $3.56^{+0.19}_{-0.26}$ |
| $\Sigma m_\nu$ [eV] | 0.06 | < 0.87 |

## VI. RESULTS WITH R16

In this section, we analyse again the models for which the tension between the 2015 Planck and Riess *et al.* 2016 [23] value of $H_0$ is less than $2\sigma$. These correspond to the scenarios where $N_{\rm eff}$ is free to vary, when we ignored the high multipole polarization data. Applying a Gaussian prior on the value of $H_0$, we obtain new constraints on the cosmological parameters (68% C.L.) for the interacting DM scenario, as shown in Table V.

We find that all the cosmological parameters are shifted towards higher values, as can be seen by comparing the results from Table V with Table I. Moreover, owing to the very well-known degeneracy between $H_0$ and $N_{\rm eff}$ (see Fig. 3), we find an indication for a dark radiation at about $2\sigma$ by imposing the R16 prior. In particular, we find $N_{\rm eff} = 3.54 \pm 0.20$ for the ΛCDM + $u$ + $N_{\rm eff}$ scenario and $N_{\rm eff} = 3.56^{+0.19}_{-0.26}$ for the ΛCDM + $u$ + $N_{\rm eff}$ + $\Sigma m_\nu$ model. A dark radiation component can be explained by the existence of some extra relic component, such as a sterile neutrino or a thermal axion [29,39,43–45]. However, in these models, an increase in the value of $N_{\rm eff}$ may not be related to the presence of an additional species. It could be related to dark matter annihilations into neutrinos as they would reheat the neutrino fluid and mimic an increase in the value of $N_{\mathrm{eff}}$ [46,47].

## VII. CONCLUSION

In the ΛCDM model, dark matter is assumed to be collisionless. This means that one arbitrarily sets the dark matter interactions to zero to interpret the CMB temperature and polarization angular power spectra and determine the cosmological parameters. Here we relaxed the collisionless assumption and studied the impact of DM-$\nu$ interactions on the cosmological parameters.

We performed a similar analysis to [21]. However this time, we used the full 2015 Planck data [36] as they include both the high and low multipoles polarization spectra and are more precise than the 2013 data. In general, we observe that the introduction of dark matter-neutrino interactions can break the existing correlation between $H_0$ and $\sigma_8$. They can increase the value of $H_0$ and simultaneously decrease the value of $\sigma_8$, thus potentially reducing the current tensions between the Planck data and other measurements. However our main conclusions are threefold.

(i) The high multipole polarization data prefer LCDM-like models, though they do also predict a smaller value for $\sigma_8$ than LCDM.

(ii) The DM-$\nu$ interactions do help to reduce the tension between the CMB and weak lensing estimates [38,41,42] of the $S_8$ value, whatever the CMB data set under consideration. This is particularly true when $N_{\mathrm{eff}}$ and/or $\Sigma m_\nu$ are kept as free parameters. However $N_{\mathrm{eff}}$ remains compatible with the standard model value, unless one also adds the Cepheids measurements.

(iii) DM-$\nu$ interactions can also help to reduce the tensions between the CMB and Cepheid measurements of the Hubble constant, if one disregards the high multipole polarization data and $N_{\mathrm{eff}}$ is introduced (performing slightly better than the $\Lambda\mathrm{CDM} + N_{\mathrm{eff}}$ model). The combination of the CMB + Cepheid data sets leads to a Hubble rate value of about $72.1^{+1.5}_{-1.7}$ km s$^{-1}$ Mpc$^{-1}$ when $N_{\mathrm{eff}}$ is free to vary (and $71.9^{+1.6}_{-1.8}$ km s$^{-1}$ Mpc$^{-1}$ when both $N_{\mathrm{eff}}$ and $\Sigma m_\nu$ are free). Under these conditions, $N_{\mathrm{eff}}$ can become as large as $N_{\mathrm{eff}} = 3.54 \pm 0.20$ or $N_{\mathrm{eff}} = 3.56^{+0.19}_{-0.26}$ if $\Sigma m_\nu$ can vary. In the latter case, we find that the sum of neutrino masses could reach up to 0.87 eV but the $\sigma_8$ parameter remains too high to reduce both the $H_0$ and $\sigma_8$ tensions simultaneously.

Finally we note that whatever the data sets used and hypothesis that we made, the DM-$\nu$ elastic scattering cross section cannot exceed $\sigma_{\mathrm{DM}} \lesssim 310^{-31}$–$610^{-31}(m_{\mathrm{DM/GeV}})$ cm$^2$.

To conclude, DM-$\nu$ interactions do not enable to solve both the $H_0$ and $\sigma_8$ tensions simultaneously, but they can reduce them slightly nonetheless, if we ignore the high multipole polarization data. Furthermore the combination of the low multipole and Cepheid data [23] show that such interactions have the potential to solve the $H_0$ tension, if we ignore the $\sigma_8$ tension. Should there be a good reason to ignore the high multipole polarization data, one could potentially establish a link between the DM abundance and the neutrino masses [48–52]. In this paper we did not perform a model selection analysis because we do not have an indication for $u$ favored over the ΛCDM model, see for example [53–56] where extensions in the neutrino sector are not favored. Anyway, the future DESI [57] and Euclid[5] surveys should be able to determine whether such relatively large interactions were present in the early Universe [37]. Such high values of the $u$ ratio would question our understanding of structure formation, as it is expected that there would be little satellite companions left in the Milky Way [10].

## ACKNOWLEDGMENTS

The authors would like to thank J. L. Bernal, M. Escudero, M. Gerbino, A. Riess, L. Verde and R. Wilkinson for very useful discussions. EDV acknowledges support from the European Research Council in the form of a Consolidator Grant with No. 681431. This research was supported in part by Perimeter Institute for Theoretical Physics. Research at Perimeter Institute is supported by the Government of Canada through Industry Canada and by the Province of Ontario through the Ministry of Economic Development and Innovation.

[5]See http://sci.esa.int/euclid/.

[1] A. A. de Laix, R. J. Scherrer, and R. K. Schaefer, Constraints of self-interacting dark matter, Astrophys. J. **452**, 495 (1995).

[2] C. Boehm, P. Fayet, and R. Schaeffer, Constraining dark matter candidates from structure formation, Phys. Lett. B **518**, 8 (2001).

[3] C. Boehm and R. Schaeffer, Constraints on dark matter interactions from structure formation: Damping lengths, Astron. Astrophys. **438**, 419 (2005).

[4] C. Boehm, A. Riazuelo, S. H. Hansen, and R. Schaeffer, Interacting dark matter disguised as warm dark matter, Phys. Rev. D **66**, 083505 (2002).

[5] C. Boehm, H. Mathis, J. Devriendt, and J. Silk, Non-linear evolution of suppressed dark matter primordial power spectra, Mon. Not. R. Astron. Soc. **360**, 282 (2005).

[6] M. Vogelsberger, J. Zavala, F. Y. Cyr-Racine, C. Pfrommer, T. Bringmann, and K. Sigurdson, ETHOS—An effective theory of structure formation: Dark matter physics as a possible explanation of the small-scale CDM problems, Mon. Not. R. Astron. Soc. **460**, 1399 (2016).

[7] F. Y. Cyr-Racine, K. Sigurdson, J. Zavala, T. Bringmann, M. Vogelsberger, and C. Pfrommer, ETHOS–an effective theory of structure formation: From dark particle physics to the matter distribution of the Universe, Phys. Rev. D **93**, 123527 (2016).

[8] J. A. Schewtschenko, R. J. Wilkinson, C. M. Baugh, C. Bœhm, and S. Pascoli, Dark matter–radiation interactions: the impact on dark matter haloes, Mon. Not. R. Astron. Soc. **449**, 3587 (2015).

[9] J. A. Schewtschenko, C. M. Baugh, R. J. Wilkinson, C. Bœhm, S. Pascoli, and T. Sawala, Dark matter–radiation interactions: the structure of Milky Way satellite galaxies, Mon. Not. R. Astron. Soc. **461**, 2282 (2016).

[10] C. Boehm, J. A. Schewtschenko, R. J. Wilkinson, C. M. Baugh, and S. Pascoli, Using the Milky Way satellites to study interactions between cold dark matter and radiation, Mon. Not. R. Astron. Soc. **445**, L31 (2014).

[11] X. l. Chen, S. Hannestad, and R. J. Scherrer, Cosmic microwave background and large scale structure limits on the interaction between dark matter and baryons, Phys. Rev. D **65**, 123515 (2002).

[12] K. Sigurdson, M. Doran, A. Kurylov, R. R. Caldwell, and M. Kamionkowski, Dark-matter electric and magnetic dipole moments, Phys. Rev. D **70**, 083501 (2004); Erratum, Phys. Rev. D **73**, 089903(E) (2006).

[13] G. Mangano, A. Melchiorri, P. Serra, A. Cooray, and M. Kamionkowski, Cosmological bounds on dark matter-neutrino interactions, Phys. Rev. D **74**, 043517 (2006).

[14] P. Serra, F. Zalamea, A. Cooray, G. Mangano, and A. Melchiorri, Constraints on neutrino—dark matter interactions from cosmic microwave background and large scale structure data, Phys. Rev. D **81**, 043507 (2010).

[15] A. D. Dolgov, S. L. Dubovsky, G. I. Rubtsov, and I. I. Tkachev, Constraints on millicharged particles from Planck data, Phys. Rev. D **88**, 117701 (2013).

[16] R. J. Wilkinson, J. Lesgourgues, and C. Boehm, Using the CMB angular power spectrum to study dark matter-photon interactions, J. Cosmol. Astropart. Phys. 04 (2014) 026.

[17] C. Dvorkin, K. Blum, and M. Kamionkowski, Constraining dark matter-baryon scattering with linear cosmology, Phys. Rev. D **89**, 023519 (2014).

[18] F. Y. Cyr-Racine and K. Sigurdson, Cosmology of atomic dark matter, Phys. Rev. D **87**, 103515 (2013).

[19] R. Diamanti, E. Giusarma, O. Mena, M. Archidiacono, and A. Melchiorri, Dark radiation and interacting scenarios, Phys. Rev. D **87**, 063509 (2013).

[20] M. Blennow, E. Fernandez-Martinez, O. Mena, J. Redondo, and P. Serra, Asymmetric dark matter and dark radiation, J. Cosmol. Astropart. Phys. 07 (2012) 022.

[21] R. J. Wilkinson, C. Boehm, and J. Lesgourgues, Constraining dark matter-neutrino interactions using the CMB and large-scale structure, J. Cosmol. Astropart. Phys. 05 (2014) 011.

[22] V. Bonvin *et al.*, H0LiCOW V. New COSMOGRAIL time delays of HE0435-1223: $H_0$ to 3.8, Mon. Not. R. Astron. Soc. **465**, 4914 (2017).

[23] A. G. Riess *et al.*, A 2.4% determination of the local value of the Hubble constant, Astrophys. J. **826**, 56 (2016).

[24] Planck Collaboration, Planck 2015 results. XI. CMB power spectra, likelihoods, and robustness of parameters, Astron. Astrophys. **594**, A11 (2016).

[25] J. Lesgourgues, The Cosmic Linear Anisotropy Solving System (CLASS) I: Overview, arXiv:1104.2932.

[26] D. Blas, J. Lesgourgues, and T. Tram, The Cosmic Linear Anisotropy Solving System (CLASS) II: Approximation schemes, J. Cosmol. Astropart. Phys. 07 (2011) 034.

[27] B. Audren, J. Lesgourgues, K. Benabed, and S. Prunet, Conservative constraints on early cosmology: An illustration of the Monte Python cosmological parameter inference code, J. Cosmol. Astropart. Phys. 02 (2013) 001.

[28] G. Mangano, G. Miele, S. Pastor, T. Pinto, O. Pisanti, and P. D. Serpico, Relic neutrino decoupling including flavor oscillations, Nucl. Phys. **B729**, 221 (2005); P. F. de Salas and S. Pastor, Relic neutrino decoupling with flavour oscillations revisited, J. Cosmol. Astropart. Phys. 07 (2016) 051.

[29] A. Heavens, R. Jimenez, and L. Verde, Standard Rulers, Candles, and Clocks from the Low-Redshift Universe, Phys. Rev. Lett. **113**, 241302 (2014); M. Archidiacono, E. Giusarma, S. Hannestad, and O. Mena, Cosmic dark radiation and neutrinos, Adv. High Energy Phys. **2013**, 1 (2013); E. Di Valentino, A. Melchiorri, and O. Mena, Dark radiation sterile neutrino candidates after Planck data, J. Cosmol. Astropart. Phys. 11 (2013) 018; E. Di Valentino, A. Melchiorri, and J. Silk, Reconciling Planck with the local value of $H_0$ in extended parameter space, Phys. Lett. B **761**, 242 (2016); S. Kumar and R. C. Nunes, Probing the interaction between dark matter and dark energy in the presence of massive neutrinos, Phys. Rev. D **94**, 123511 (2016); T. Tram, R. Vallance, and V. Vennin, Inflation model selection meets dark radiation, J. Cosmol. Astropart. Phys. 01 (2017) 046; E. Di Valentino and F. R. Bouchet, A comment on power-law inflation with a dark radiation component, J. Cosmol. Astropart. Phys. 10 (2016) 011; E. Di Valentino and L. Mersini-Houghton, Testing predictions of the quantum landscape multiverse 2: The exponential inflationary potential, J. Cosmol. Astropart. Phys. 03 (2017) 020.

[30] E. Di Valentino, E. Giusarma, O. Mena, A. Melchiorri, and J. Silk, Cosmological limits on neutrino unknowns versus low redshift priors, Phys. Rev. D **93**, 083527 (2016).

[31] F. Simpson, R. Jimenez, C. Pena-Garay, and L. Verde, Strong Bayesian evidence for the normal neutrino hierarchy, J. Cosmol. Astropart. Phys. 06 (2017) 029.

[32] T. Schwetz, K. Freese, M. Gerbino, E. Giusarma, S. Hannestad, M. Lattanzi, O. Mena, and S. Vagnozzi, Comment on "Strong evidence for the normal neutrino hierarchy", arXiv:1703.04585.

[33] A. J. Long, M. Raveri, W. Hu, and S. Dodelson, Neutrino mass priors for cosmology from random matrices, arXiv:1711.08434 [Phys. Rev. D (to be published)].

[34] S. Gariazzo, M. Archidiacono, P. F. de Salas, O. Mena, C. A. Ternes, and M. Tórtola, Neutrino masses and their ordering: Global data, priors and models, arXiv:1801.04946.

[35] Planck Collaboration, Planck 2015 results. XV. Gravitational lensing, Astron. Astrophys. **594**, A15 (2016).

[36] Planck Collaboration, Planck 2015 results. XIII. Cosmological parameters, Astron. Astrophys. **594**, A13 (2016).

[37] M. Escudero, O. Mena, A. C. Vincent, R. J. Wilkinson, and C. Bœhm, Exploring dark matter microphysics with galaxy surveys, J. Cosmol. Astropart. Phys. 09 (2015) 034.

[38] H. Hildebrandt *et al.*, KiDS-450: Cosmological parameter constraints from tomographic weak gravitational lensing, Mon. Not. R. Astron. Soc. **465**, 1454 (2017).

[39] E. Giusarma, E. Di Valentino, M. Lattanzi, A. Melchiorri, and O. Mena, Relic neutrinos, thermal axions and cosmology in early 2014, Phys. Rev. D **90**, 043507 (2014).

[40] N. MacCrann, J. Zuntz, S. Bridle, B. Jain, and M. R. Becker, Cosmic discordance: Are Planck CMB and CFHTLenS weak lensing measurements out of tune?, Mon. Not. R. Astron. Soc. **451**, 2877 (2015); E. Di Valentino, A. Melchiorri, and J. Silk, Beyond six parameters: Extending ΛCDM, Phys. Rev. D **92**, 121302 (2015).

[41] C. Heymans *et al.*, CFHTLenS: The Canada-France-Hawaii Telescope Lensing Survey, Mon. Not. R. Astron. Soc. **427**, 146 (2012).

[42] T. Erben *et al.*, CFHTLenS: The Canada-France-Hawaii Telescope Lensing Survey—Imaging data and catalogue products, Mon. Not. R. Astron. Soc. **433**, 2545 (2013).

[43] E. Di Valentino, E. Giusarma, M. Lattanzi, O. Mena, A. Melchiorri, and J. Silk, Cosmological axion and neutrino mass constraints from Planck 2015 temperature and polarization data, Phys. Lett. B **752**, 182 (2016).

[44] E. Di Valentino, S. Gariazzo, M. Gerbino, E. Giusarma, and O. Mena, Dark radiation and inflationary freedom after Planck 2015, Phys. Rev. D **93**, 083523 (2016).

[45] M. Archidiacono, E. Calabrese, and A. Melchiorri, The case for dark radiation, Phys. Rev. D **84**, 123008 (2011).

[46] C. Boehm, M. J. Dolan, and C. McCabe, A lower bound on the mass of cold thermal dark matter from Planck, J. Cosmol. Astropart. Phys. 08 (2013) 041.

[47] C. Boehm, M. J. Dolan, and C. McCabe, Increasing Neff with particles in thermal equilibrium with neutrinos, J. Cosmol. Astropart. Phys. 12 (2012) 027.

[48] A. Arhrib, C. Bœhm, E. Ma, and T. C. Yuan, Radiative model of neutrino mass with neutrino interacting MeV dark matter, J. Cosmol. Astropart. Phys. 04 (2016) 049.

[49] C. Boehm, Y. Farzan, T. Hambye, S. Palomares-Ruiz, and S. Pascoli, Is it possible to explain neutrino masses with scalar dark matter?, Phys. Rev. D **77**, 043516 (2008).

[50] E. Ma, Verifiable radiative seesaw mechanism of neutrino mass and dark matter, Phys. Rev. D **73**, 077301 (2006).

[51] Y. Farzan, A minimal model linking two great mysteries: neutrino mass and dark matter, Phys. Rev. D **80**, 073009 (2009).

[52] Y. Farzan, S. Pascoli, and M. A. Schmidt, AMEND: A model explaining neutrino masses and dark matter testable at the LHC and MEG, J. High Energy Phys. 10 (2010) 111.

[53] S. M. Feeney, H. V. Peiris, and L. Verde, Is there evidence for additional neutrino species from cosmology?, J. Cosmol. Astropart. Phys. 04 (2013) 036.

[54] L. Verde, S. M. Feeney, D. J. Mortlock, and H. V. Peiris, (Lack of) cosmological evidence for dark radiation after Planck, J. Cosmol. Astropart. Phys. 09 (2013) 013.

[55] B. Leistedt, H. V. Peiris, and L. Verde, No New Cosmological Concordance with Massive Sterile Neutrinos, Phys. Rev. Lett. **113**, 041301 (2014).

[56] A. Heavens, Y. Fantaye, E. Sellentin, H. Eggers, Z. Hosenie, S. Kroon, and A. Mootoovaloo, No Evidence for Extensions to the Standard Cosmological Model, Phys. Rev. Lett. **119**, 101301 (2017).

[57] M. Levi *et al.* (DESI Collaboration), The DESI Experiment, a whitepaper for Snowmass 2013, arXiv:1308.0847.